

Generative Pseudo-Labeling for Pre-Ranking with LLMs

Junyu Bi*
Alibaba Group
Beijing, China
bijunyu.bjy@taobao.com

Xinting Niu*
Alibaba Group
Beijing, China
niuxinting.nxt@alibaba-inc.com

Daixuan Cheng†
Renmin University
Beijing, China
daixuancheng6@gmail.com

Kun Yuan‡
Alibaba Group
Beijing, China
yuankun.yuan@taobao.com

Tao Wang
Alibaba Group
Beijing, China
wt439443@taobao.com

Binbin Cao
Alibaba Group
Beijing, China
simon.cbb@taobao.com

Jian Wu
Alibaba Group
Beijing, China
joshuawu.wujian@taobao.com

Yuning Jiang
Alibaba Group
Beijing, China
mengzhu.jyn@taobao.com

Abstract

Pre-ranking is a critical stage in industrial recommendation systems, tasked with efficiently scoring thousands of recalled items for downstream ranking. A key challenge is the train–serving discrepancy: pre-ranking models are trained only on exposed interactions, yet must score all recalled candidates—including unexposed items—during online serving. This mismatch not only induces severe sample selection bias but also degrades generalization, especially for long-tail content. Existing debiasing approaches typically rely on heuristics (e.g., negative sampling) or distillation from biased rankers, which either mislabel plausible unexposed items as negatives or propagate exposure bias into pseudo-labels. In this work, we propose **Generative Pseudo-Labeling (GPL)**, a framework that leverages large language models (LLMs) to generate unbiased, content-aware pseudo-labels for unexposed items, explicitly aligning the training distribution with the online serving space. By offline generating user-specific interest anchors and matching them with candidates in a frozen semantic space, GPL provides high-quality supervision without adding online latency. Deployed in a large-scale production system, GPL improves click-through rate by 3.07%, while significantly enhancing recommendation diversity and long-tail item discovery.

CCS Concepts

• Information systems → Retrieval models and ranking;

*Both authors contributed equally to this research.

†Work done during an internship at Alibaba Group.

‡Corresponding author.

Permission to make digital or hard copies of all or part of this work for personal or classroom use is granted without fee provided that copies are not made or distributed for profit or commercial advantage and that copies bear this notice and the full citation on the first page. Copyrights for components of this work owned by others than the author(s) must be honored. Abstracting with credit is permitted. To copy otherwise, to republish, to post on servers or to redistribute to lists, requires prior specific permission and/or a fee. Request permissions from permissions@acm.org.

Conference acronym 'XX, Woodstock, NY

© 2018 Copyright held by the owner/author(s). Publication rights licensed to ACM.

ACM ISBN 978-1-4503-XXXX-X/2018/06

<https://doi.org/XXXXXXX.XXXXXXX>

Keywords

Recommender system; Sample selection bias; Large language model.

ACM Reference Format:

Junyu Bi, Xinting Niu, Daixuan Cheng, Kun Yuan, Tao Wang, Binbin Cao, Jian Wu, and Yuning Jiang. 2018. Generative Pseudo-Labeling for Pre-Ranking with LLMs. In *Proceedings of Make sure to enter the correct conference title from your rights confirmation email (Conference acronym 'XX)*. ACM, New York, NY, USA, 12 pages. <https://doi.org/XXXXXXX.XXXXXXX>

1 Introduction

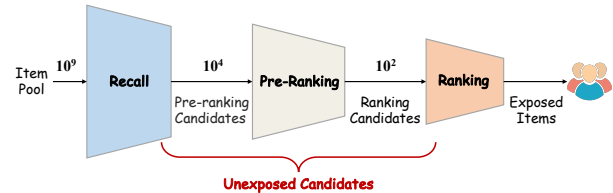


Figure 1: Illustration of the cascade-based architecture in recommender systems. The unexposed candidates are items retrieved in early stages but discarded.

In large-scale industrial recommendation systems, cascade architectures—comprising candidate recall, pre-ranking, ranking, and re-ranking—are widely used [42] (Fig. 1). The pre-ranking stage scores thousands of recalled items with lightweight models, forwarding only the top candidates to ranking. However, this early filtering exacerbates sample selection bias (SSB) [24]: during training, pre-ranking models rely solely on exposed interactions (e.g., clicks or purchases), yet at inference must score all recalled items—including unexposed ones lacking feedback. This train–inference distribution shift harms generalization, especially for long-tail or novel items, promoting over-recommendation of popular content, reinforcing information cocoons, and reducing diversity [37].

Research on mitigating SSB in recommendation systems has pursued several directions. Early methods treat unexposed items as negatives via binary classification or negative sampling [26], but

this introduces false negatives and worsens exposure bias. Randomized content delivery [22] yields unbiased feedback yet is costly and risks user experience, limiting scalability [7]. Teacher–student frameworks distill pseudo-labels from ranking models, but inherit exposure bias since teachers are trained only on exposed data, hurting generalization to unexposed items. Adversarial domain adaptation aligns exposed and unexposed distributions [40], yet often suffers from instability and dependence on biased interaction graphs [38]. Meanwhile, large language models (LLMs) have demonstrated strong semantic priors and been applied to recommendation tasks—such as metadata enrichment, intent elicitation, candidate generation [39], and synthetic feedback [44]. However, no existing work leverages LLM semantics to infer relevance for unexposed items, leaving a gap in addressing SSB during pre-ranking.

To bridge the train–inference gap and mitigate exposure bias, we propose **Generative Pseudo-Labeling (GPL)**, a two-stage framework that aligns pre-ranker training with the full recall set encountered at serving time. **Firstly**, GPL generates content-aware pseudo-labels for unexposed items. It begins by tokenizing items into hierarchical *semantic identifiers* (SIDs) using a frozen multimodal encoder and a Residual Quantized VAE—ensuring representations are grounded in content, not biased interactions. A fine-tuned large language model then predicts future SIDs from user histories, which are decoded into *interest-anchors*. Relevance scores are computed by matching these anchors with candidates in the frozen multimodal space, and further calibrated via an uncertainty-aware weighting scheme that accounts for semantic coherence, historical consistency, and LLM confidence. **Secondly**, the pre-ranker is trained on a unified objective that jointly optimizes observed interactions and the calibrated pseudo-labels through a confidence-weighted loss. Crucially, all LLM inference and pseudo-label generation are performed offline and cached per user, imposing zero latency overhead during online serving. Our contributions are as follows:

- We propose GPL, to the best of our knowledge the first framework that leverages LLMs to address SSB in pre-ranking by explicitly aligning the training supervision with the online serving space, enabling robust generalization to unexposed and long-tail items. GPL overcomes the limitation of relying solely on exposed data, alleviates SSB, and enables the modeling of a broader and more diverse spectrum of user interests.
- We design an efficient two-step pseudo-labeling process for unexposed items, which on the one hand reduces reliance on exposed samples through generative interest-anchors creation, and on the other hand leverages multimodal information to further mitigate exposure and popularity biases.
- The method has been deployed on a large-scale industrial recommendation platform, where it achieved a 3.07% increase in click-through rate (CTR) in online A/B testing, and simultaneously enhancing recommendation diversity while alleviating long-tail distribution bias.

2 Related Work

In industrial recommender systems, the pre-ranking stage quickly filters large candidate sets but often suffers from SSB due to training exclusively on exposed interactions. Meanwhile, LLMs have

recently demonstrated strong potential in recommendation via semantic understanding and knowledge reasoning. We thus review related work along two directions: (1) SSB mitigation methods in recommender systems, and (2) LLM applications in recommendation.

2.1 Mitigating SSB in Recommender Systems

A first family of approaches reshapes the training data. Simple binary classification treats all unexposed items as negatives [3, 11], and random or hard negative sampling attempts to narrow the gap between training and serving distributions [45]. These strategies are easy to deploy but inevitably introduce false negatives, reinforcing popularity and exposure biases and suppressing promising yet unexposed items. An alternative approach aimed at actively collecting unbiased user feedback via randomized content delivery strategies can be used for training corrective models or for knowledge transfer [22]. However, exploration traffic is costly and risky, and high-variance propensities and user experience degradation often undermine their practicality in production [7].

To bypass expensive exploration, teacher–student transfer is widely used. Knowledge distillation leverages scores from the downstream ranker as soft supervision to train the front-end model on unexposed data [30], either using the continuous scores directly or converting them into more reliable binary targets via confidence-aware filtering and thresholding [6]. A persistent bottleneck is the fidelity of the pseudo-labels: ranker scores for the unexposed items are frequently miscalibrated and inherit exposure bias.

Another line of research recasts SSB as a source–target shift. Adversarial domain adaptation aims to align the feature distributions of exposed and unexposed data using a discriminator and gradient reversal while simultaneously optimizing the task objective [19]. Recognizing that not all unexposed samples are equally informative, some research identify informative unexposed items via random walks or structural cues on user–item graphs and then apply adversarial alignment on this subset [21]. But they still only depend on actual labels derived from biased logs and the adversarial alignment is unstable and hard to scale [38].

2.2 Applications of LLMs for Recommendation

The advent of large language models (LLMs) has introduced a new paradigm in recommender systems by enabling the use of rich semantic priors and weak supervision signals derived from item content and context. Unlike traditional recommenders that depend heavily on explicit feedback, LLMs can reason about items and user intents through language understanding and world knowledge, offering supervision less prone to exposure bias. This capability has been applied to diverse tasks: *metadata enrichment* [14] refines or expands item attributes; *intent elicitation* [20] uncovers latent preferences via natural-language interaction; *candidate generation* [4] proposes semantically relevant items beyond standard retrieval; and *synthetic feedback* [44] simulates user preferences to augment sparse training data. These advances demonstrate LLMs’ potential to inject content-aware, bias-resilient signals—especially valuable when behavioral data is limited or skewed.

However, existing applications of LLMs in recommendation do not specifically focus on mining *unexposed items*—a critical yet

supervision-scarce subset of the recall set. Positioned within this landscape, our work fuses semantic patterns from the LLM with observed user interactions through confidence-aware calibration. This process enriches the unexposed domain with semantically grounded supervision that reflects both content relevance and behavioral signals, obviating the need for expensive unbiased logging or complex joint end-to-end training. As a result, we obtain a practical, plug-and-play solution that seamlessly integrates into independently trained cascade stages to effectively mitigate sample selection bias (SSB).

3 Methodology

3.1 Problem Formulation

We consider a recommendation setting with a set of users \mathcal{U} and an item corpus \mathcal{H} . The goal is to learn a relevance scoring function $f: \mathcal{U} \times \mathcal{H} \rightarrow \mathbb{R}$ that ranks items for each user, with higher scores indicating greater interest. In practice, supervision comes only from *exposed interactions*:

$$\mathcal{D}_e = \{(u, h, y_{u,h}) \mid u \in \mathcal{U}, h \in S_u \subseteq \mathcal{H}, y_{u,h} \in \{0, 1\}\},$$

where S_u is the set of items shown to user u , and $y_{u,h}$ denotes binary feedback (e.g., click). However, exposure is biased toward popular items, limiting the model’s ability to discover long-tail content.

To address this, we additionally leverage *unexposed candidates*:

$$\mathcal{D}_u = \{(u, h) \mid u \in \mathcal{U}, h \in \bar{S}_u \subseteq \mathcal{H} \setminus S_u\},$$

which consists of items retrieved by upstream stages (e.g., recall) but not exposed to the user. Though lacking ground-truth labels, these pairs are semantically plausible and offer opportunities for discovery. The core challenge is to assign reliable pseudo-labels $r_{u,h} \in [0, 1]$ to $(u, h) \in \mathcal{D}_u$. We tackle this via a content-aware preference estimator (Section 3.3.3) and train f with a joint objective:

$$\min_f \mathcal{L}_{al}(\mathcal{D}_e) + \lambda \mathcal{L}_{pl}(\mathcal{D}_u), \quad (1)$$

where \mathcal{L}_{al} and \mathcal{L}_{pl} are losses on actual and pseudo labels, respectively, and $\lambda > 0$ balances their contributions.

3.2 Overview of the Framework

To overcome exposure bias, we generate high-quality pseudo-labels for unexposed items by leveraging large language models in a discrete semantic space. Specifically, we tokenize user histories into semantic identifiers (SIDs) via a multimodal RQ-VAE, then use a fine-tuned LLM to predict the next likely SID and decode diverse interest anchors. These anchors are aligned with candidate items in the multimodal space to produce content-aware relevance scores, which are calibrated by uncertainty-aware weighting. The calibrated pseudo-labels are jointly optimized with observed interactions, enabling the ranker to discover long-tail items while preserving robustness.

3.3 Pseudo Labels Generation

In this section, we leverage a fine-tuned large language model to generate pseudo-labels for unexposed items. By decoding semantic identifiers of likely next interactions and aligning them in a multimodal space, our method produces content-aware relevance scores without relying on historical exposure.

3.3.1 Tokenization of User Behaviors. To enable symbolic reasoning with LLMs while avoiding exposure bias, we tokenize items into discrete semantic identifiers (SIDs) using only content information. Each item h is first encoded by a frozen pre-trained multimodal encoder f_e , which fuses textual descriptions and visual features into a unified embedding $\mathbf{e}_{mm} = f_e(h) \in \mathbb{R}^d$. These embeddings are precomputed for all items and stored in a shared multimodal embedding pool, allowing any module in the pipeline to retrieve an item’s representation via efficient lookup. The encoder remains frozen to preserve general-purpose semantics and prevent contamination from biased interactions.

We train a Residual Quantized Variational Autoencoder (RQ-VAE) [12, 31] on the full item corpus, using \mathbf{e}_{mm} as reconstruction targets. The RQ-VAE learns L hierarchical codebooks that quantize \mathbf{e}_{mm} into a sequence of discrete indices $s = (s^{(1)}, \dots, s^{(L)})$, defined as the item’s SID. Critically, training relies solely on reconstruction and commitment losses, ensuring the token space reflects intrinsic content rather than exposure patterns. During training, we build a lookup table mapping each observed SID to its item ID, enabling exact resolution at inference. User interaction histories are converted into SID sequences for LLM processing. This content-only tokenizer yields a discrete space that is semantically grounded, adapted to the platform’s item distribution, and inherently decoupled from historical feedback bias—making it particularly suitable for long-tail and cold-start scenarios. More implementation details of multimodal encoder and RQ-VAE are provided in Appendix A.

3.3.2 Interest-Anchors Generation. Given the tokenized user history H_u , we adapt a pre-trained open-source LLM to predict future interests in the semantic identifier (SID) space. The model input (see Appendix B for details) is constructed as:

$$X_u = \text{concat}(\text{tokens}(T), \text{tokens}(H_u)), \quad (2)$$

where T is a natural-language instruction prompt. The LLM is trained exclusively on sequences of positively interacted items (e.g., clicks or purchases), converted to their SIDs. To mitigate popularity bias inherited from interaction logs, we apply frequency-based downsampling to the top 10% most frequent items in the training corpus. Each interaction involving such an item is retained with probability inversely proportional to its frequency [43]. This strategy reduces the dominance of head items while preserving sufficient signal for stable LLM training.

To balance adaptation efficacy and computational efficiency, we employ Low-Rank Adaptation (LoRA) [13] (rank=8): trainable low-rank matrices are injected into the query and value projections of all attention layers, while the original LLM parameters remain frozen. This reduces trainable parameters by over 99% and preserves the model’s pre-trained semantic knowledge. Training follows the Next Token Prediction (NTP) objective. The last SID in H_u is masked as the target, and the loss minimizes the negative log-likelihood over all hierarchical levels:

$$\mathcal{L}_{ntp} = \sum_{l=1}^L -\log P\left(s_{\text{next}}^{(l)} \mid X_u, s_{\text{next}}^{(1:l-1)}; \theta\right), \quad (3)$$

where θ denotes the trainable parameters.

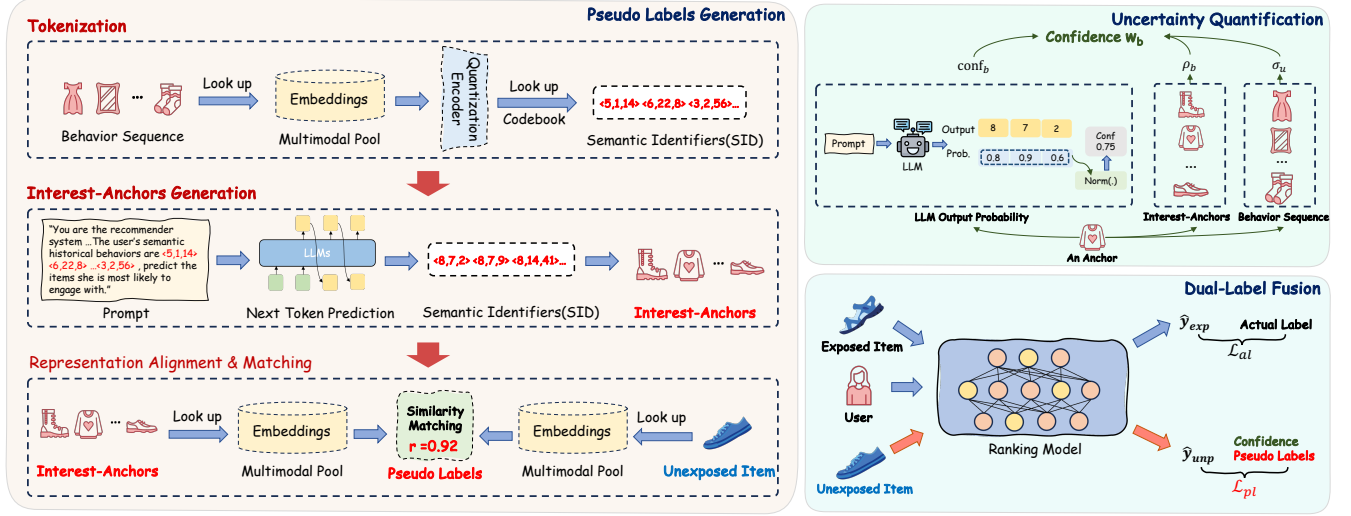


Figure 2: Overview of the GPL framework. For each user, interest anchors are generated offline via an LLM in a discrete semantic space and matched with unexposed candidates to produce pseudo-labels. These are calibrated by confidence weights based on semantic coherence, historical consistency, and generation uncertainty. In the Dual-Label Fusion stage, pseudo-labeled unexposed items are combined with exposed items bearing actual labels to jointly train the pre-ranking model.

At inference, we perform hierarchical beam search [5] with width B to decode diverse SID candidates $\mathcal{S}_{\text{beam}} = \{s_1, \dots, s_B\}$. Each generated SID s_b is resolved to a real item a_b via the precomputed lookup table built during RQ-VAE training. Empirically, over 98.5% of generated SIDs exist in the table (measured on a validation cohort), confirming strong coverage of plausible future interactions. For the rare out-of-vocabulary cases (<1.5%), we fall back to nearest-neighbor retrieval in the frozen multimodal embedding space. The final interest-anchor set is:

$$A_u = \{a_1, \dots, a_B\}. \quad (4)$$

Crucially, during training and inference, we apply a causal attention mask [33] over the entire sequence, ensuring that predictions at each position depend only on past and present tokens—not future ones. This enforces a strict temporal order and prevents information leakage, enabling the model to better capture sequential dynamics in user behavior.

3.3.3 Representation Alignment & Matching. We employ a large pre-trained multimodal encoder f_e to project both interest anchors and unexposed items into a shared semantic space. The encoder fuses heterogeneous inputs—such as product images, titles, price, category, and metadata—to produce rich, content-aware embeddings. By aligning user interests and candidates in this semantically coherent space, relevance scoring relies on content-based matching rather than interaction history, explicitly mitigating exposure and popularity biases and enhancing discoverability of long-tail items with rich content but sparse interactions.

Given these aligned representations, the relevance score for a user–item pair (u, h) is computed as follows. For each anchor $a_i \in A_u$, we compute cosine similarity $\cos(f_e(a_i), f_e(h))$. While a naive approach might average over all anchors, uniform averaging assumes equal relevance—an assumption often violated when

A_u contains noisy or weakly related candidates due to LLM generation errors or embedding distortions [17, 41]. Prior work in multi-interest modeling shows that max-pooling is more robust, as it emphasizes the strongest semantic match while suppressing irrelevant signals [16]. Following this principle, we define:

$$r_{u,h} = \text{Sigmoid}\left(\frac{\max_{a_i \in A_u} \cos(f_e(a_i), f_e(h))}{\tau}\right) \in (0, 1), \quad (5)$$

where $\tau > 0$ is a temperature hyperparameter tuned on a validation cohort to optimize ranking calibration. This score serves as the pseudo-label for (u, h) in the subsequent *dual-label fusion* stage.

3.4 Dual-Label Fusion

3.4.1 Uncertainty Quantification. To assess the reliability of LLM-generated interest anchors, we quantify uncertainty along three orthogonal dimensions:

- **Semantic Dispersion:** Given the B anchor embeddings $\{f_e(a_b)\}_{b=1}^B$, we compute their pairwise dissimilarity:

$$\sigma_u = \frac{1}{B(B-1)} \sum_{i \neq j} (1 - \cos(f_e(a_i), f_e(a_j))). \quad (6)$$

A high σ_u indicates unstable generation and reflects epistemic uncertainty.

- **Historical Consistency:** For each anchor a_b , we measure its alignment with the user’s historical interactions $\{h_m\}_{m=1}^M$:

$$\rho_b = \frac{1}{M} \sum_{m=1}^M \cos(f_e(a_b), f_e(h_m)). \quad (7)$$

- **LLM-Intrinsic Confidence:** For anchor a_b corresponding to SID s_b , we compute its average log-probability along the decoding

path [2]:

$$\text{conf}_b = \frac{1}{L} \sum_{l=1}^L \log P(s_b^{(l)} | X_u, s_b^{(1:l-1)}; \theta). \quad (8)$$

These three uncertainty signals capture complementary aspects of anchor reliability. **Semantic Dispersion** (σ_u) reflects the *epistemic uncertainty* of the LLM: if generated anchors are semantically inconsistent, the model is likely uncertain about the user’s intent. **Historical Consistency** (ρ) measures *behavioral plausibility*: an anchor that aligns well with the user’s past interactions is more likely to represent a genuine preference. **LLM-Intrinsic Confidence** (conf) captures the *aleatoric uncertainty* from the generation process itself—low log-probability indicates the LLM is extrapolating beyond its training distribution. By jointly considering these dimensions, our weighting scheme down-weights anchors that are either internally inconsistent, behaviorally implausible, or generated with low confidence, thereby improving the quality of pseudo-labels.

We first calculate the anchor-level confidence weight for anchor a_b as:

$$\tilde{w}_b = \exp(\lambda_1 \rho_b) \cdot \exp(\lambda_2 \cdot \text{conf}_b), \quad (9)$$

and then apply user-level calibration based on semantic dispersion σ_u , which quantifies the coherence of generated anchors. The final confidence weight is obtained via softmax normalization:

$$w_b = \exp(-\sigma_u) \cdot \frac{\exp(\tilde{w}_b)}{\sum_{b'=1}^B \exp(\tilde{w}_{b'})}, \quad (10)$$

where the term $\exp(-\sigma_u)$ uniformly down-weights all anchors for users with high semantic dispersion, reflecting reduced overall reliability.

3.4.2 Joint Optimization. We train the lightweight pre-ranker f with a unified probabilistic objective. For exposed data \mathcal{D}_e , we use standard binary cross-entropy (BCE) with hard labels $y_{u,h} \in \{0, 1\}$:

$$\mathcal{L}_{\text{al}} = -\frac{1}{|\mathcal{D}_e|} \sum_{(u,h) \in \mathcal{D}_e} [y_{u,h} \log \hat{y}_{u,h} + (1 - y_{u,h}) \log(1 - \hat{y}_{u,h})], \quad (11)$$

where $\hat{y}_{u,h} = f(u, h)$.

For unexposed data \mathcal{D}_u , we first calculate the confidence weight for each pair (u, h) : let $a^* = \arg \max_{a_i \in A_u} \cos(f_c(a_i), f_c(h))$ be the anchor yielding the strongest match. The sample-level confidence weight is then $w_{u,h} = w_{a^*}$, as defined in Eq (10). The pseudo-label loss is then defined as a confidence-weighted BCE:

$$\mathcal{L}_{\text{pl}} = -\frac{1}{|\mathcal{D}_u|} \sum_{(u,h) \in \mathcal{D}_u} w_{u,h} [r_{u,h} \log \hat{y}_{u,h} + (1 - r_{u,h}) \log(1 - \hat{y}_{u,h})]. \quad (12)$$

The final training objective combines both actual labels and pseudo labels in a unified manner:

$$\mathcal{L} = \mathcal{L}_{\text{al}} + \lambda \mathcal{L}_{\text{pl}}, \quad (13)$$

where λ balances the contribution of pseudo-labels. In practice, we select λ and τ jointly via online A/B testing to maximize click-through rate (CTR) and long-tail coverage. All components except the pre-ranker f remain frozen during training.

3.5 Industrial Deployment Details

The pseudo-label generation pipeline is entirely offline and imposes zero runtime overhead on the production serving system. All components operate in a batch setting, leveraging precomputed static features to maximize efficiency.

Specifically, multimodal embeddings for all items are generated offline during system initialization, L2-normalized, and cached in a distributed feature store. After initialization, the multimodal encoder is invoked only for newly added items (e.g., fresh products uploaded daily), while embeddings for existing items are reused without recomputation. This incremental update strategy ensures that heavy multimodal inference—typically involving vision and language backbones—is performed infrequently and at minimal scale.

The only large-model computation occurs during LLM-based interest-anchors generation. By generating user-level interest anchors (rather than per-candidate predictions), a single LLM forward pass suffices per user’s request—reducing inference calls by approximately sixfold compared to naive per-candidate generation. This stage runs on a dedicated offline cluster: using 96 NVIDIA H20 GPUs, we complete inference for one day’s user traffic within six hours.

Subsequent steps—including item ID lookup, similarity matching, and confidence weighting—are lightweight and executed on standard CPU workers. The final output is a set of pseudo-labeled training samples, which are merged with observed interactions to train the lightweight pre-ranker. As a result, GPL integrates seamlessly into existing pre-ranking pipelines without requiring any modifications to the online architecture, enabling safe deployment and rapid iteration.

4 Experiments

4.1 Setup

4.1.1 Datasets. We evaluate our method on two datasets.

Industrial Dataset: We construct an industrial-scale dataset comprising authentic, high-quality user interaction logs collected from *Taobao*¹. The dataset spans a continuous 14-day period and includes approximately 200 million users and 20 million items, yielding around 30 billion interaction records. The first 13 days of data are used for training, and the final day is reserved for validation. Following the production serving pipeline, the *exposed dataset* consists of items actually displayed to users, while the *unexposed dataset* contains items retrieved during the recall stage but filtered out before display.

Taobao-MM²: Taobao-MM [36] is an official large-scale recommendation dataset that incorporates multimodal item representations. In our experiments, we utilize all 8.79 million users and 35.4 million items. User-side features include user ID, age, and gender; item-side features comprise item ID and category. For each user, all items with which they have not interacted are treated as unexposed candidates.

4.1.2 Baselines & Implementation Details. In line with recent studies, we benchmark our method against several representative strategies that exploit unexposed items. Since public datasets lack

¹<https://www.taobao.com>

²<https://huggingface.co/datasets/TaoBao-MM/Taobao-MM>

Table 1: Overall performance comparison on the Taobao industrial dataset and Taobao-MM dataset.

| Dataset | Industrial Dataset | | | | | Taobao-MM | | | | |
|------------|--------------------|---------------|---------------|---------------|---------------|---------------|---------------|---------------|---------------|---------------|
| Method | HR@3 | HR@5 | HR@10 | AUC | GAUC | HR@3 | HR@5 | HR@10 | AUC | GAUC |
| BC | 0.4863 | 0.5850 | 0.7611 | 0.7096 | 0.6098 | 0.4412 | 0.5405 | 0.7122 | 0.6854 | 0.5912 |
| KD | 0.4938 | 0.6247 | 0.8181 | 0.7110 | 0.6114 | 0.4498 | 0.5721 | 0.7516 | 0.6892 | 0.5945 |
| TL | 0.4905 | 0.6283 | 0.8102 | 0.7106 | 0.6107 | 0.4470 | 0.5735 | 0.7495 | 0.6885 | 0.5938 |
| MUDA | 0.4972 | 0.6299 | 0.8268 | 0.7116 | 0.6110 | 0.4522 | 0.5788 | 0.7602 | 0.6898 | 0.5940 |
| UKD | 0.5061 | 0.6477 | 0.8301 | 0.7145 | 0.6218 | 0.4610 | 0.5925 | 0.7714 | 0.6962 | 0.6015 |
| UECF | 0.5216 | 0.6699 | 0.8585 | 0.7246 | 0.6313 | 0.4824 | 0.6210 | 0.8055 | 0.7055 | 0.6124 |
| SIDA | 0.5143 | 0.6626 | 0.8499 | 0.7210 | 0.6241 | 0.4705 | 0.6105 | 0.7922 | 0.7001 | 0.6045 |
| DAMCAR | 0.5191 | 0.6650 | 0.8498 | 0.7206 | 0.6277 | 0.4788 | 0.6152 | 0.7954 | 0.7022 | 0.6088 |
| GPL | 0.5254 | 0.6777 | 0.8680 | 0.7299 | 0.6338 | 0.4912 | 0.6324 | 0.8198 | 0.7112 | 0.6175 |

ranking models, we train a ranking model on exposed dataset to serve as the teacher for those baselines that require pseudo-labels.

- **Binary Classification (BC):** A fundamental baseline that trains the model directly on exposed data, treating user clicks as positive labels while ignoring the inherent selection bias.
- **Knowledge Distillation (KD):** This approach uses the ranking model’s prediction scores as soft pseudo-labels to train the front-end model [26].
- **Transfer Learning (TL):** This method fine-tunes the item embedding tower with pseudo-labels on unexposed data while freezing the user tower [25].
- **Modified Unsupervised Domain Adaptation (MUDA):** It introduces a threshold-based pseudo-label filtering mechanism that converts the continuous scores of the ranking model into reliable binary labels for training [34].
- **Adversarial Domain Adaptation:** This line of work aligns the distributions of exposed and unexposed data by training a domain discriminator with a gradient reversal layer [8]. We instantiate this category with two strong baselines, i.e., **UKD** [40] and **UECF** [19].
- **Selective Adversarial Domain Adaptation:** These methods identify informative unexposed items as a target domain via random walks on a user–item bipartite graph and assign robust labels to them through adversarial domain adaptation. We select two SOTA methods **SIDA** [35] and **DAMCAR** [21] as baselines.

All models are trained using the Adam optimizer for dense parameters and Adagrad for sparse parameters, with an initial learning rate of 1×10^{-3} . Qwen2.5-0.5B [1] is adopted for user interest-anchor generation, and the impact of different LLM backbones is further explored in Section 4.4 and Table 3.

For Industrial Dataset, the input features include user ID, gender, item ID, item category, and the user behavior sequence. Item information is encoded using a frozen CLIP model [27]. The RQ-VAE is configured with three quantization layers, each equipped with a codebook of 8,192 entries.

For Taobao-MM Dataset, we adopt SCL-based multimodal embeddings [29] to train the RQ-VAE, which employs a two-layer quantization structure with 200 codebook entries per layer. The input features consist of user ID, age, gender, item ID, item category, and the user behavior sequence.

4.1.3 Metrics. In offline experiments, we evaluate top- K recommendation quality using **Hit Rate (HR@ K)** with $K \in \{3, 5, 10\}$, where HR@ K is calculated on exposed samples for each user. We also assess overall ranking performance via **AUC** and **Group AUC (GAUC)** [46]. GAUC computes the average of per-user AUCs to mitigate bias from highly active users and better reflect the typical user experience. Additionally, to measure pseudo-label quality, we generate pseudo-labels for exposed items and compute the AUC between these pseudo-labels and real user feedback, denoted as **AUC***.

In online experiments, we measure utility and user engagement. Utility metrics—**Item Page Views (IPV)**, **Click-Through Rate (CTR)**, and **Click-Through Conversion Rate (CTCVR)**—capture the system’s effectiveness in driving actions and revenue. Engagement is assessed via **UV3** (users scrolling through >200 items per session) and **Dwell Time (DT)**, which reflect interaction depth and duration. Higher engagement suggests stronger interest and improved long-term retention.

4.2 Overall Performance Comparison

Table 1 compares **GPL** with a range of baselines on our industrial dataset, yielding three key insights.

First, the **BC** baseline—trained exclusively on exposed interactions—achieves the lowest performance across all metrics. This stark underperformance empirically validates a central premise of our work: unexposed candidates are not merely negative samples but contain rich signals about user preferences. By ignoring them, BC discards potentially relevant items that were never shown due to system limitations, thereby reinforcing exposure bias and limiting recommendation diversity.

Second, pseudo-labeling methods (**KD**, **TL**, **MUDA**) remain sub-optimal. Their teacher models, trained only on exposed data, inherit and propagate exposure bias into pseudo-labels, creating a feedback loop that amplifies popularity bias and suppresses discovery of novel interests.

Third, **GPL** significantly outperforms all baselines, including advanced domain adaptation approaches (**UKD**, **UECF**, etc.). Unlike coarse distribution alignment, **GPL** generates user-specific interest anchors via an LLM and assigns uncertainty-calibrated relevance scores to individual unexposed items. The consistent gains confirm

Table 2: Ablation study of GPL on the Industrial Dataset.

| Method | HR | | AUC | GAUC | AUC* |
|------------------------------|---------------|---------------|---------------|---------------|---------------|
| | @3 | @10 | | | |
| w/o Semantic IDs | 0.5158 | 0.8592 | 0.7221 | 0.6252 | 0.6194 |
| w/o Multimodal Encoder | 0.5094 | 0.8540 | 0.7219 | 0.6236 | 0.6167 |
| w/o Max-Pooling | 0.5072 | 0.8537 | 0.7184 | 0.6220 | 0.6023 |
| w/o Confidence | 0.5215 | 0.8639 | 0.7223 | 0.6279 | - |
| w/o Semantic Dispersion | 0.5233 | 0.8656 | 0.7269 | 0.6294 | - |
| w/o Historical Consistency | 0.5244 | 0.8667 | 0.7281 | 0.6317 | - |
| w/o LLM-Intrinsic Confidence | 0.5237 | 0.8662 | 0.7275 | 0.6304 | - |
| w/o Actual Labels | 0.3687 | 0.6933 | 0.6239 | 0.5863 | - |
| GPL | 0.5254 | 0.8680 | 0.7299 | 0.6338 | 0.6275 |

that semantically grounded, dual-label supervision—combining observed clicks with LLM-informed signals—enables more robust and diverse recommendations.

In summary, Table 1 highlights that: (i) exploiting unexposed candidates is essential; (ii) naive pseudo-labeling from an exposure-trained ranker is inadequate; and (iii) integrating observed clicks with semantically generated, uncertainty-aware supervision on unexposed items enables GPL to achieve state-of-the-art performance across all offline metrics.

4.3 Ablation Study

To evaluate the contributions of key components in GPL, we conducted an ablation study under identical experimental settings. By systematically removing or replacing modules, we quantified each component’s impact on recommendation performance using the industrial-scale dataset. Several variants were constructed:

- **w/o Semantic IDs:** The RQ-VAE tokenization is removed. The LLM is trained to directly predict the next raw item ID from historical item ID sequences.
- **w/o Multimodal Encoder:** The frozen multimodal encoder f_e is replaced with standard learnable ID embeddings from the item embedding layer.
- **w/o Max-Pooling:** Max-pooling over anchor similarities is replaced with mean-pooling. Pseudo-labels are computed as the average (rather than maximum) cosine similarity between an unexposed item and all interest anchors.
- **w/o Confidence:** The confidence-aware weighting is disabled. All pseudo-labels are assigned uniform weight $w_{u,h} = 1$ in \mathcal{L}_{pl} , assuming equal reliability.
- **w/o Semantic Dispersion:** The semantic dispersion term (σ_u) is excluded from the confidence weight computation.
- **w/o Historical Consistency:** The historical consistency term (ρ) is removed from the confidence weight computation.
- **w/o LLM-Intrinsic Confidence:** The LLM-intrinsic confidence term (conf) is dropped from the confidence weight computation.
- **w/o Actual Labels:** The actual-label loss \mathcal{L}_{al} (Eq (1)) is removed. The model is trained solely on pseudo-labels.

As shown in Table 2, every component of GPL is essential: removing any module leads to a consistent performance drop across all metrics.

Effect of pseudo label quality. In Table 2, the first three variants (rows 1–3) assess the contribution of each component in pseudo-label generation. Notably, all components are essential: removing

Table 3: Performance comparison across LLM backbones.

| LLM-backbone | Gflops/token | AUC | AUC* |
|--------------|--------------|--------|--------|
| Qwen2.5-0.5B | 0.30 | 0.7299 | 0.6257 |
| Qwen2.5-1.8B | 0.98 | 0.7317 | 0.6286 |
| Qwen2.5-7B | 5.25 | 0.7354 | 0.6333 |

any one results in a significant drop in AUC*, indicating degraded pseudo-label quality, which in turn leads to reduced performance of the final ranking model. Among these, the *w/o Max-Pooling* variant—replacing max-pooling with mean-pooling—causes the largest degradation, reducing HR@3 by 0.182. This supports the intuition that focusing on the single most relevant interest anchor yields more discriminative signals than averaging across all anchors.

Impact of the Confidence. Rows 4–7 in Table 2 evaluate the role of confidence weighting, which does not affect pseudo-label quality directly but is crucial during joint optimization. Specifically, the *w/o Confidence* variant reduces HR@3 from 0.5254 to 0.5215, confirming that calibrating the LLM’s raw outputs is essential for effective pseudo-labeling. We further dissect the confidence weighting mechanism into its three uncertainty components. Among them, removing Semantic Dispersion causes the largest performance drop, indicating that LLM-generated interest anchors exhibit substantial user-wise variability in semantic coherence. Explicitly modeling this dispersion is therefore critical for robust uncertainty estimation.

Importance of Actual Label. The most severe degradation occurs in the *w/o Actual Labels* setting, where HR@3 plummets from 0.5254 to 0.3687. This dramatic drop underscores that supervision from observed interactions is indispensable—not only for providing ground-truth signals but also for stabilizing training and preventing model drift in the presence of noisy pseudo-labels.

4.4 Model Configuration Study

In this section, we evaluate the impact of different LLM backbones and tokenization strategies to justify the cost-effectiveness and architectural choices of GPL.

Effect of LLM Model Size. We compare three Qwen2.5 variants [1] for interest anchor generation: 0.5B, 1.8B, and 7B. As shown in Table 3, larger models improve both the final AUC on real user interactions and the pseudo-label quality, measured by AUC*, which is the AUC between pseudo-labels and real feedback on exposed items. The 7B model achieves the highest AUC of 73.54 and AUC* of 63.33 but requires 5.25 Gflops/token. In contrast, the 0.5B model attains a competitive AUC of 72.99 with only 0.30 Gflops/token and AUC* = 62.57. **Although AUC* is lower than AUC, indicating imperfect pseudo-labels, it remains sufficiently aligned with user feedback to effectively guide training.** Given Taobao’s massive traffic scale, the 0.5B variant offers the best trade-off between performance and inference efficiency.

Sensitivity to the balance weight λ in joint optimization. As shown in the Figure 3-(a), varying λ exhibits a clear unimodal trend. Small λ values collapse training into exposure-only supervision, reducing interest coverage and lowering AUC and HR@3, whereas

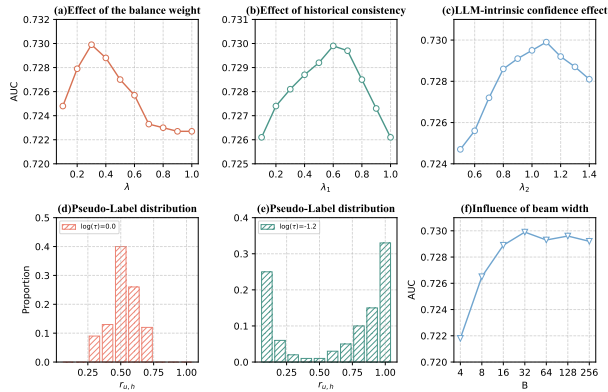


Figure 3: We conduct a parameter sensitivity analysis of the balance weight λ , the historical consistency weight λ_1 , and the LLM-intrinsic confidence weight λ_2 . The effects of the beam size B and temperature τ are also investigated. AUC performance is plotted for all parameters across their respective ranges.

large values over-trust generated labels, amplifying noise and distribution shift, again harming performance. The optimum occurs at moderate λ (0.1–1.0 in our setting), where actual and estimated supervision are balanced. Without confidence weighting, the optimum shifts lower and the right tail drops more steeply, showing that it mitigates noise from unreliable anchors, broadens λ 's stable range, and raises the performance ceiling.

Analysis of the historical consistency weight λ_1 and LLM-intrinsic confidence weight λ_2 . In Eq (9), the historical consistency weight λ_1 measures the similarity between the generated interest anchor and the user's historical behavior. A larger λ_1 encourages selection of anchors more aligned with past interactions, yielding more stable generation. However, as shown in Figure 3-(b), when $\lambda_1 > 0.6$, the model's AUC begins to decline. An excessively high λ_1 overly favors historically similar anchors, limiting selection diversity and exacerbating the sample selection bias (SSB) problem. In contrast, the LLM-intrinsic confidence weight λ_2 reflects the LLM's inherent uncertainty. As illustrated in Figure 3-(c), peak AUC performance is achieved at $\lambda_2 = 1.1$. Further increasing λ_2 beyond this point amplifies LLM hallucinations, leading to unstable and overly divergent interest anchors.

Impact of temperature τ on pseudo-label sharpness. The temperature coefficient τ critically shapes the pseudo-label distribution, as Figure 3-(d) and (e). Lower values of τ sharpen the distribution toward a Bernoulli-like form, better approximating the true posterior and yielding a clearer separation between positive and negative samples. However, in this low-temperature regime, the sigmoid function saturates, compressing probabilities near 0 or 1. This suppresses fine-grained distinctions within each class—among positives or negatives—thereby discarding dense intra-class information essential for representation learning. Empirically, peak AUC performance is achieved at $\log(\tau) \approx -1.2$, balancing label clarity and information retention.

The effect of beam size B . The right column of Figure 3-(f) shows the effect of anchor set size. Increasing B from small to moderate



Figure 4: Fine-Grained Online A/B Analysis of GPL vs. Base-line. (a) Relative CTR lift (%) and absolute PVR change (percentage points, pt) across historical page-view (PV) buckets. (b) Category distribution of exposed items.

steadily boosts metrics by enriching interest coverage and increasing the likelihood that at least one anchor matches each unexposed candidate. Gains saturate beyond a threshold ($N = 32$ by default), after which extra anchors mostly contribute near-duplicates or lower-quality candidates, yielding diminishing or slightly negative returns. Without confidence weighting, performance peaks earlier and declines as N grows, indicating that larger sets introduce more noise unless moderated by uncertainty-aware weights. Confidence weighting not only raises the peak performance but also delays saturation, making larger N beneficial.

4.5 Online Experiments.

4.5.1 Overall Effectiveness in Online Deployment. To rigorously assess GPL's real-world effectiveness and scalability, we deployed it in the pre-ranking stage of Taobao's "Guess What You Like" homepage feed and conducted a two-week online A/B test with hundreds of millions of daily active users. As shown in Table 4, GPL achieves consistent gains across all metrics: CTR (+3.07%) and IPV (+3.53%) improve significantly, confirming more engaging recommendations. The +2.51% lift in CTCVR indicates these clicks are high-quality, driving more purchases and business value. Gains in UV3 (+1.50%) and Dwell Time (+2.16%) further suggest users find the content more compelling, leading to deeper exploration and longer sessions.

4.5.2 Impact on SSB and Generalization. To validate our hypothesis that GPL mitigates selection bias and enhances discovery, we conduct a fine-grained online analysis (Figure 4).

First, we partition items into seven buckets by historical Page Views (PV). Figure 4(a) shows that GPL achieves increasing CTR lift for lower-PV (long-tail) items, indicating its ability to surface relevant but previously overlooked content. The pseudo-labels provide crucial supervision to counteract popularity bias.

Second, we examine category diversity. The baseline concentrates 70.80% of recommendations in the top-10 categories, leaving only 29.20% for the remaining 100+ categories. In contrast, GPL reduces the dominant share to 45.91%—a >35% relative drop. The w/o Multimodal Encoder variant lies in between, suggesting two complementary effects: (1) LLM-based interest generation reduces

Table 4: Online A/B Test Performance Gains.

| Method | IPV | CTR | CTCVR | UV3 | DT |
|--------|--------|--------|--------|--------|--------|
| GPL | +3.53% | +3.07% | +2.51% | +1.50% | +2.16% |

reliance on exposure history and expands coverage; (2) alignment with a content-rich multimodal space further debiases representation, enabling broader cross-category exploration.

5 Conclusion

In this paper, we presented GPL, a framework that jointly leverages actual labels from exposed interactions and pseudo labels for unexposed candidates generated via an LLM-driven preference estimation module. By converting simulated feedback into explicit supervision, GPL alleviates exposure bias, improves data efficiency, and models a broader spectrum of user interests. Deployed on a large-scale industrial platform, our approach achieved a 3.07% CTR lift in online A/B testing, demonstrating its practical value and scalability.

References

- [1] Jinze Bai, Shuai Bai, Yunfei Chu, Zeyu Cui, Kai Dang, Xiaodong Deng, Yang Fan, Wenbin Ge, Yu Han, Fei Huang, et al. 2023. Qwen technical report. *arXiv preprint arXiv:2309.16609* (2023).
- [2] Tom B. Brown, Benjamin Mann, Nick Ryder, Melanie Subbiah, Jared Kaplan, Prafulla Dhariwal, Arvind Neelakantan, Pranav Shyam, Girish Sastry, Amanda Askell, Sandhini Agarwal, Ariel Herbert-Voss, Gretchen Krueger, Tom Henighan, Rewon Child, Aditya Ramesh, Daniel M. Ziegler, Jeffrey Wu, Clemens Winter, Christopher Hesse, Mark Chen, Eric Sigler, Mateusz Litwin, Scott Gray, Benjamin Chess, Jack Clark, Christopher Berner, Sam McCandlish, Alec Radford, Ilya Sutskever, and Dario Amodei. 2020. Language Models are Few-Shot Learners. In *Advances in Neural Information Processing Systems 33: Annual Conference on Neural Information Processing Systems 2020, NeurIPS 2020, December 6–12, 2020, virtual*. <https://proceedings.neurips.cc/paper/2020/hash/1457c0d6bfc4967418bfb8ac142f64a-Abstract.html>
- [3] Jiawei Chen, Hande Dong, Xiang Wang, Fuli Feng, Meng Wang, and Xiangnan He. 2023. Bias and debias in recommender system: A survey and future directions. *ACM Transactions on Information Systems* 41, 3 (2023), 1–39.
- [4] Yingpeng Du, Di Luo, Rui Yan, Xiaopei Wang, Hongzhi Liu, Hengshu Zhu, Yang Song, and Jie Zhang. 2024. Enhancing job recommendation through llm-based generative adversarial networks. In *Proceedings of the AAAI conference on artificial intelligence*, Vol. 38. 8363–8371.
- [5] Markus Freitag and Yaser Al-Onaizan. 2017. Beam search strategies for neural machine translation. *arXiv preprint arXiv:1702.01806* (2017).
- [6] Feng Gao, Xin Zhou, Yinning Shao, Yue Wu, Jiahua Gao, Yujian Ren, Fengyang Qi, Ruochen Deng, and Jie Liu. 2025. Both Supply and Precision: Sample Debias and Ranking Consistency Joint Learning for Large Scale Pre-Ranking System. In *Proceedings of the AAAI Conference on Artificial Intelligence*, Vol. 39. 11672–11680.
- [7] Jingyue Gao, Shuguang Han, Han Zhu, Siran Yang, Yuning Jiang, Jian Xu, and Bo Zheng. 2023. Rec4ad: A free lunch to mitigate sample selection bias for ads ctr prediction in taobao. In *Proceedings of the 32nd ACM International Conference on Information and Knowledge Management*. 4574–4580.
- [8] Ian J Goodfellow, Jean Pouget-Abadie, Mehdi Mirza, Bing Xu, David Warde-Farley, Sherjil Ozair, Aaron Courville, and Yoshua Bengio. 2014. Generative adversarial nets. *Advances in neural information processing systems* 27 (2014).
- [9] Kaiming He, Haoqi Fan, Yuxin Wu, Saining Xie, and Ross Girshick. 2020. Momentum contrast for unsupervised visual representation learning. In *Proceedings of the IEEE/CVF conference on computer vision and pattern recognition*. 9729–9738.
- [10] Ruining He, Lukasz Heldt, Lichan Hong, Raghunandan Keshavan, Shifan Mao, Nikhil Mehta, Zhengyang Su, Alicia Tsai, Yueqi Wang, Shao-Chuan Wang, et al. 2025. Plum: Adapting pre-trained language models for industrial-scale generative recommendations. *arXiv preprint arXiv:2510.07784* (2025).
- [11] Xiangnan He, Yang Zhang, Fuli Feng, Chonggang Song, Lingling Yi, Guohui Ling, and Yongdong Zhang. 2023. Addressing confounding feature issue for causal recommendation. *ACM Transactions on Information Systems* 41, 3 (2023), 1–23.
- [12] Yupeng Hou, Zhankui He, Julian McAuley, and Wayne Xin Zhao. 2023. Learning vector-quantized item representation for transferable sequential recommenders. In *Proceedings of the ACM Web Conference 2023*. 1162–1171.
- [13] Edward J Hu, Yelong Shen, Phillip Wallis, Zeyuan Allen-Zhu, Yuanzhi Li, Shean Wang, Lu Wang, Weizhu Chen, et al. 2022. Lora: Low-rank adaptation of large language models. *ICLR* 1, 2 (2022), 3.
- [14] Jun Hu, Wenwen Xia, Xiaolu Zhang, Chilin Fu, Weichang Wu, Zhaoxin Huan, Ang Li, Zuoli Tang, and Jun Zhou. 2024. Enhancing sequential recommendation via llm-based semantic embedding learning. In *Companion Proceedings of the ACM Web Conference 2024*. 103–111.
- [15] Doyoung Lee, Chiheon Kim, Saehoon Kim, Minsu Cho, and Wook-Shin Han. 2022. Autoregressive image generation using residual quantization. In *Proceedings of the IEEE/CVF conference on computer vision and pattern recognition*. 11523–11532.
- [16] Chao Li, Zhiyuan Liu, Mengmeng Wu, Yuchi Xu, Huan Zhao, Pipei Huang, Guoliang Kang, Qiwei Chen, Wei Li, and Dik Lun Lee. 2019. Multi-interest network with dynamic routing for recommendation at Tmall. In *Proceedings of the 28th ACM international conference on information and knowledge management*. 2615–2623.
- [17] Dongsheng Li, Chao Chen, Zhilin Gong, Tun Lu, Stephen M Chu, and Ning Gu. 2019. Collaborative filtering with noisy ratings. In *Proceedings of the 2019 SIAM International Conference on Data Mining*. SIAM, 747–755.
- [18] Junnan Li, Dongxu Li, Silvio Savarese, and Steven Hoi. 2023. Blip-2: Bootstrapping language-image pre-training with frozen image encoders and large language models. In *International conference on machine learning*. PMLR, 19730–19742.
- [19] Xuanlin Li, Xiangyu Cai, Hao Peng, Jia Duan, Wei Wang, Zehua Zhang, Changping Peng, Zhangang Lin, Ching Law, and Jingping Shao. 2025. An Unbiased Entire-Space Causal Framework for Click-Through Rate Estimation in Pre-Ranking. In *Companion Proceedings of the ACM on Web Conference 2025*. 306–314.
- [20] Zhaorui Lian, Binzong Geng, Xiyu Chang, Yu Zhang, Ke Ding, Ziyu Lyu, Guanghu Yuan, Chengming Li, Min Yang, Zhaoxin Huan, et al. 2025. EGRec: Leveraging Generative Rich Intents for Enhanced Recommendation with Large Language Models. In *Companion Proceedings of the ACM on Web Conference 2025*. 1113–1117.
- [21] Jiaye Lin, Qing Li, Guorui Xie, Zhongxu Guan, Yong Jiang, Ting Xu, Zhong Zhang, and Peilin Zhao. 2024. Mitigating Sample Selection Bias with Robust Domain Adaption in Multimedia Recommendation. In *Proceedings of the 32nd ACM International Conference on Multimedia*. 7581–7590.
- [22] Dugang Liu, Pengxiang Cheng, Zinan Lin, Xiaolian Zhang, Zhenhua Dong, Rui Zhang, Xiuqiang He, WeiKe Pan, and Zhong Ming. 2023. Bounding system-induced biases in recommender systems with a randomized dataset. *ACM Transactions on Information Systems* 41, 4 (2023), 1–26.
- [23] Shicong Liu, Hongtao Lu, and Junru Shao. 2015. Improved Residual Vector Quantization for High-dimensional Approximate Nearest Neighbor Search. *CoRR* abs/1509.05195 (2015).
- [24] Zohreh Ovaisi, Ragib Ahsan, Yifan Zhang, Kathryn Vasilaky, and Elena Zheleva. 2020. Correcting for selection bias in learning-to-rank systems. In *Proceedings of the web conference 2020*. 1863–1873.
- [25] Sinno Jialin Pan and Qiang Yang. 2010. A Survey on Transfer Learning. *IEEE Transactions on Knowledge and Data Engineering* 22, 10 (2010), 1345–1359. doi:10.1109/TKDE.2009.191
- [26] Jiarui Qin, Jiachen Zhu, Bo Chen, Zhirong Liu, Weiwen Liu, Ruiming Tang, Rui Zhang, Yong Yu, and Weinan Zhang. 2022. Rankflow: Joint optimization of multi-stage cascade ranking systems as flows. In *Proceedings of the 45th International ACM SIGIR Conference on Research and Development in Information Retrieval*. 814–824.
- [27] Alec Radford, Jong Wook Kim, Chris Hallacy, Aditya Ramesh, Gabriel Goh, Sandhini Agarwal, Girish Sastry, Amanda Askell, Pamela Mishkin, Jack Clark, et al. 2021. Learning transferable visual models from natural language supervision. In *International conference on machine learning*. PMLR, 8748–8763.
- [28] Ali Razavi, Aaron Van den Oord, and Oriol Vinyals. 2019. Generating diverse high-fidelity images with vq-vae-2. *Advances in neural information processing systems* 32 (2019).
- [29] Xiang-Rong Sheng, Feifan Yang, Litong Gong, Biao Wang, Zhangming Chan, Yujing Zhang, Yueyao Cheng, Yong-Nan Zhu, Tiezheng Ge, Han Zhu, et al. 2024. Enhancing Taobao Display Advertising with Multimodal Representations: Challenges, Approaches and Insights. In *Proceedings of the 33rd ACM International Conference on Information and Knowledge Management*. 4858–4865.
- [30] Haoyuan Song, Yibowen Zhao, Yixin Zhang, Hongxu Chen, and Lizhen Cui. 2025. Knowledge Distillation Based Recommendation Systems: A Comprehensive Survey. *Electronics* 14, 8 (2025), 1538.
- [31] Aaron Van Den Oord, Oriol Vinyals, et al. 2017. Neural discrete representation learning. *Advances in neural information processing systems* 30 (2017).
- [32] Aäron van den Oord, Oriol Vinyals, and Koray Kavukcuoglu. 2017. Neural Discrete Representation Learning. In *Advances in Neural Information Processing Systems 30: Annual Conference on Neural Information Processing Systems 2017, December 4–9, 2017, Long Beach, CA, USA*. 6306–6315.
- [33] Ashish Vaswani, Noam Shazeer, Niki Parmar, Jakob Uszkoreit, Llion Jones, Aidan N Gomez, Lukasz Kaiser, and Illia Polosukhin. 2017. Attention is all you need. *Advances in neural information processing systems* 30 (2017).
- [34] Yuan Wang, Peifeng Yin, Zhiqiang Tao, Hari Venkatesan, Jin Lai, Yi Fang, and PJ Xiao. 2023. An empirical study of selection bias in pinterest ads retrieval. In *Proceedings of the 29th ACM SIGKDD Conference on Knowledge Discovery and Data Mining*. 5174–5183.
- [35] Jianping Wei, Yujie Zhou, Zhengwei Wu, and Ziqi Liu. 2024. Enhancing pre-ranking performance: Tackling intermediary challenges in multi-stage cascading recommendation systems. In *Proceedings of the 30th ACM SIGKDD Conference on Knowledge Discovery and Data Mining*. 5950–5958.

- [36] Bin Wu, Feifan Yang, Zhangming Chan, Yu-Ran Gu, Jiawei Feng, Chao Yi, Xiang-Rong Sheng, Han Zhu, Jian Xu, Mang Ye, and Bo Zheng. 2025. MUSE: A Simple Yet Effective Multimodal Search-Based Framework for Lifelong User Interest Modeling. arXiv:2512.07216 [cs.LG] <https://arxiv.org/abs/2512.07216>
- [37] Yunjia Xi, Muyan Weng, Wen Chen, Chao Yi, Dian Chen, Gaoyang Guo, Mao Zhang, Jian Wu, Yuning Jiang, Qingwen Liu, et al. 2025. Bursting filter bubble: Enhancing serendipity recommendations with aligned large language models. In *Proceedings of the 31st ACM SIGKDD Conference on Knowledge Discovery and Data Mining V. 2*. 5059–5070.
- [38] Yue Xing, Qifan Song, and Guang Cheng. 2021. On the algorithmic stability of adversarial training. *Advances in neural information processing systems* 34 (2021), 26523–26535.
- [39] Xiaochuan Xu, Zeqiu Xu, Peiyang Yu, and Jiani Wang. 2025. Enhancing user intent for recommendation systems via large language models. In *International Conference on Artificial Intelligence and Machine Learning Research (CAIMLR 2024)*, Vol. 13635. SPIE, 46–54.
- [40] Zixuan Xu, Penghui Wei, Weimin Zhang, Shaoguo Liu, Liang Wang, and Bo Zheng. 2022. Ukd: Debiasing conversion rate estimation via uncertainty-regularized knowledge distillation. In *Proceedings of the ACM Web Conference 2022*. 2078–2087.
- [41] Kaike Zhang, Qi Cao, Fei Sun, Yunfan Wu, Shuchang Tao, Huawei Shen, and Xueqi Cheng. 2023. Robust recommender system: a survey and future directions. *Comput. Surveys* (2023).
- [42] Shuai Zhang, Lina Yao, Aixin Sun, and Yi Tay. 2019. Deep learning based recommender system: A survey and new perspectives. *ACM computing surveys (CSUR)* 52, 1 (2019), 1–38.
- [43] Yang Zhang, Fuli Feng, Xiangnan He, Tianxin Wei, Chonggang Song, Guohui Ling, and Yongdong Zhang. 2021. Causal intervention for leveraging popularity bias in recommendation. In *Proceedings of the 44th international ACM SIGIR conference on research and development in information retrieval*. 11–20.
- [44] Zijian Zhang, Shuchang Liu, Ziru Liu, Rui Zhong, Qingpeng Cai, Xiangyu Zhao, Chunxu Zhang, Qidong Liu, and Peng Jiang. 2025. Llm-powered user simulator for recommender system. In *Proceedings of the AAAI Conference on Artificial Intelligence*, Vol. 39. 13339–13347.
- [45] Binglei Zhao, Houying Qi, Guang Xu, Mian Ma, Xiwei Zhao, Feng Mei, Sulong Xu, and Jinghe Hu. 2025. A Hybrid Cross-Stage Coordination Pre-ranking Model for Online Recommendation Systems. In *Companion Proceedings of the ACM on Web Conference 2025*. 621–630.
- [46] Guorui Zhou, Xiaoqiang Zhu, Chenru Song, Ying Fan, Han Zhu, Xiao Ma, Yanghui Yan, Junqi Jin, Han Li, and Kun Gai. 2018. Deep Interest Network for Click-Through Rate Prediction. In *Proceedings of the 24th ACM SIGKDD International Conference on Knowledge Discovery & Data Mining*. 1059–1068.

A Details of Tokenization

A.1 Multimodal Encoding

To construct a unified, content-rich representation for each item, we leverage a frozen vision-language foundation model and a light-weight fusion module trained solely on intrinsic item attributes—without any user interaction signals.

Specifically, we use a pretrained CLIP model [27] with both its text and image encoders frozen. The textual metadata (title, category, and description) is encoded into $x_{\text{text}} \in \mathbb{R}^d$, while the product image (resized to 224×224) is encoded into $x_{\text{img}} \in \mathbb{R}^d$.

To fuse these modalities, we adopt a Q-Former [18] with n_q learnable query tokens. The Q-Former performs cross-attention over the concatenated features $[x_{\text{text}}, x_{\text{img}}]$ and outputs fused queries \tilde{Q} , which are mean-pooled to produce the final multimodal embedding $\mathbf{e}_{\text{mm}} \in \mathbb{R}^d$. Crucially, the Q-Former is trained **only on the item corpus itself** using a symmetric InfoNCE objective [9]:

$$\mathcal{L}_{\text{align}} = \text{InfoNCE}(\tilde{Q}, x_{\text{img}}) + \text{InfoNCE}(\tilde{Q}, x_{\text{text}}),$$

which aligns text and image views without external supervision.

Once trained, \mathbf{e}_{mm} for every item is precomputed and stored in a shared *multimodal embedding pool*. This pool serves as the sole source of item representations throughout the pipeline: the RQ-VAE uses it as reconstruction targets, the LLM-based anchor generator retrieves from it for matching, and the final ranker accesses it via lookup—all without further updating the encoder or fusion module. This design ensures that all downstream components operate on a consistent, bias-free, and semantically grounded content representation.

A.2 RQ-VAE Training Procedure

To construct a discrete, content-grounded token space for LLM-based reasoning, we train a Residual Quantized Variational Autoencoder (RQ-VAE) [15] using only the frozen multimodal embeddings \mathbf{e}_{mm} from the shared embedding pool as reconstruction targets—**without any user interaction or behavioral supervision**.

The RQ-VAE encoder maps \mathbf{e}_{mm} to a latent vector $e \in \mathbb{R}^d$, which is then quantized through L hierarchical residual codebook levels. At each level l , a codeword $z^{(l)}$ is selected via nearest-neighbor search from a learnable codebook, and the residual $e^{(l+1)} = e^{(l)} - z^{(l)}$ is passed to the next level. The final quantized representation is $\hat{z} = \sum_{l=1}^L z^{(l)}$, which the decoder reconstructs as $\hat{\mathbf{e}}_{\text{mm}}$.

The training objective combines reconstruction and commitment losses at each level:

$$\mathcal{L}_{\text{RQ-VAE}} = \|\mathbf{e}_{\text{mm}} - \hat{\mathbf{e}}_{\text{mm}}\|_2^2 + \beta \sum_{l=1}^L \|e^{(l)} - \text{sg}(z^{(l)})\|_2^2,$$

where $\beta = 0.25$ and $\text{sg}(\cdot)$ denotes stop-gradient. Codebooks are updated via exponential moving average (EMA) with decay factor 0.99 [28], ensuring stable and efficient quantization.

Upon convergence, each item’s quantized code sequence $s = (s^{(1)}, \dots, s^{(L)})$ —its *semantic identifier* (SID)—is recorded in a lookup table that maps SIDs back to original items. This enables exact resolution during LLM inference and ensures that the discrete token space remains **semantically faithful to content, well-calibrated to the item distribution, and free from exposure bias**.

A.3 Impact of Co-occurrence Contrastive Loss

We investigated the effect of incorporating a co-occurrence contrastive loss [10] during RQ-VAE training, which encourages items frequently co-interacted by users to have similar SIDs. As expected, this alignment improves consistency between pseudo-labels and *observed* user feedback on exposed items: the AUC computed over \mathcal{D}_e (denoted AUC*) increases by 0.003 compared to the content-only variant.

However, this gain comes at a significant cost. The behavior-aware token space becomes skewed toward popular item clusters, reducing semantic resolution for long-tail items and suppressing diverse interest patterns that deviate from historical exposure. Consequently, when the pseudo-labels are used to train the final ranker f , overall ranking performance on the full candidate set degrades—measured by a **0.007 drop in AUC**.

This trade-off reveals a key insight: while behavior-aligned tokenization better fits *past interactions*, it harms generalization to *unexposed and long-tail candidates*. Our content-only tokenizer sacrifices marginal fit on observed data to achieve substantially better discovery capability—a design choice aligned with our goal of mitigating exposure bias and enhancing recommendation diversity.

B Sample Construction of Next Token Prediction

Following the construction of the SID vocabulary via RQ-VAE, we structure training and inference samples at the user level to capture long-term intent and latent preferences. Each sample integrates three key components:

- **User Behavior Sequences:** For each user, the most recent m session-based interactions are chronologically aggregated into a unified sequence H_u , with each item represented by its SID to support next-SID prediction.
- **User Information:** Demographic attributes (e.g., age, gender, location) and preference signals (e.g., favored brands, categories, and price ranges).
- **Item Metadata Corpus:** Each SID is linked to rich item metadata—including first- and second-level categories, brand, price, and recommendation timestamp—providing semantic grounding that enables the LLM to leverage its pre-trained knowledge for interpreting discrete SIDs.

Crucially, whenever a user generates a new interaction, we immediately update their behavior history and construct a new training sample. This dynamic sampling strategy not only ensures the model continuously adapts to evolving user interests and captures short-term intent with minimal latency, but also avoids storing redundant historical snapshots—thereby reducing the total number of training samples and improving both storage and computational efficiency in large-scale deployment.

To investigate the impact of prompt formulation on GPL’s performance, we conduct controlled experiments by varying the amount of user and item information provided to the LLM. We first design a *basic prompt* that contains only the **user behavior sequences**:

Basic prompt

Now, you are the recommender system for the Taobao homepage. The user’s semantic historical behaviors are H_u . Please predict the item the user is most likely to engage with in the future.

For contrast, we construct a *detailed prompt* that further incorporates **user information** and **item metadata corpus**:

Detailed prompt

You are the recommender system for the Taobao homepage. The target user is a 28-year-old female from Shanghai, China, with VIP membership and a preference for Chinese-language content. The user’s semantic historical behaviors are H_u . Recently, she has viewed summer dresses, added skincare kits to her cart, and purchased Bluetooth earphones. In her most recent sessions, she clicked on smart home lamps and browsed yoga mats, with browsing activity peaking between 8 PM and 10 PM on her iPhone 14 Pro. Her top preferred categories include skincare, fashion accessories, and fitness equipment, with a preferred price range of 100–500 RMB. She favors brands such as L’Oréal, Xiaomi, and Nike, and prefers minimalist styles and pastel colors. She also shows interest in niche organic skincare brands. The current date is July 15, 2025, during the Summer Sale season, with sunny weather and a temperature of 32°C in Shanghai. Active promotions include limited-time discounts on fitness gear. Based on the above profile, H_u , and contextual information, predict the items she is most likely to engage with in the near future.

Experimental results consistently demonstrate that richer prompts lead to stronger performance across offline metrics, with notable uplifts of 0.25% in HR@3 and 0.14% in GAUC. These observations confirm that prompt engineering is an important factor for fully realizing GPL’s potential. In practice, incorporating rich, structured user context into LLM prompts can significantly enhance recommendation quality, particularly in scenarios characterized by diverse or sparse interaction patterns. All experiments in section 4 are relay on the detailed prompt.

C Analysis of Tokenization Strategy

We investigate how the choice of item tokenization method and codebook configuration affects the quality of interest anchors.

Table 5: Analysis of quantization methods and codebooks.

| Configuration | AUC |
|-----------------------------------|--------------|
| <i>Quantization Method</i> | |
| Multiple VQ | 71.71 |
| RQ-Kmeans | 72.69 |
| RQ-VAE | 72.99 |
| <i>Codebook Structure</i> | |
| 2×32768 | 72.51 |
| 3×8192 | 72.99 |

First, we compare RQ-VAE against alternative quantization approaches: *Multiple VQ* [32] and *RQ-Kmeans* [23]. As shown in Table 5, RQ-VAE consistently outperforms both baselines. Unlike Multiple VQ—which quantizes each level independently—RQ-VAE employs a hierarchical residual structure that better captures the coarse-to-fine semantic granularity inherent in multimodal item representations.

Second, we examine the impact of codebook hierarchy depth. We compare a 2-level configuration (2×32768 codewords) with our default 3-level setup (3×8192 codewords). Although both yield comparable total vocabulary sizes, the 3-level variant achieves higher AUC. This suggests that a deeper hierarchy with smaller per-level codebooks provides a more structured and learnable sequence for the LLM to model user behavior dynamics.